ORIGINAL PAPER

An approximate technique for determining in closed form the response transition probability density function of diverse nonlinear/hysteretic oscillators

Antonios T. Meimaris · Ioannis A. Kougioumtzoglou · Athanasios A. Pantelous · Antonina Pirrotta

Abstract An approximate analytical technique is developed for determining, in closed form, the transition probability density function (PDF) of a general class of first-order stochastic differential equations (SDEs) with nonlinearities both in the drift and in the diffusion coefficients. Specifically, first, resorting to the Wiener path integral most probable path approximation and utilizing the Cauchy–Schwarz inequality yields a closed-form expression for the system response PDF, at practically zero computational cost. Next, the accuracy of this approximation is enhanced by proposing a more general PDF form with additional parameters to be determined. This is done by relying on the associated Fokker–Planck operator to formulate and solve an error minimization problem. Besides the mathematical merit of the derived closed-form approximate PDFs, an additional significant advantage of the technique relates to the fact that it can be readily coupled with a stochastic averaging treatment of second-order SDEs governing the dynamics of diverse stochastically excited nonlinear/hysteretic oscillators. In this regard, it is shown that the technique is capable of determining approximately the response amplitude transition PDF of a wide range of nonlinear oscillators, including hysteretic systems following the Preisach versatile modeling. Several numerical examples are considered for demonstrating the reliability and computational efficiency of the technique. Comparisons with pertinent Monte Carlo simulation data are provided as well.

Keywords Nonlinear stochastic dynamics · Path integral · Cauchy–Schwarz inequality · Fokker–Planck equation · Stochastic differential equations

A. T. Meimaris · A. A. Pantelous
Department of Econometrics and Business Statistics, Monash University, Clayton, VIC 3800, Australia
e-mail: Antonios.Meimaris@monash.edu

A. A. Pantelous
e-mail: Athanasios.Pantelous@monash.edu

I. A. Kougioumtzoglou (✉)
Department of Civil Engineering and Engineering Mechanics, Columbia University, New York, NY 10027, USA
e-mail: ikougioum@columbia.edu

A. Pirrotta
Department of Mathematical Sciences, University of Liverpool, Peach Street, Liverpool L69 7ZL, UK
e-mail: antonina.pirrotta@unipa.it

A. Pirrotta
Dipartimento di Ingegneria, Universitá degli Studi di Palermo, Viale delle Scienze, Ed. 8, 90128 Palermo, Italy

1 Introduction

Although Monte Carlo simulation (MCS) has been the most versatile tool for solving stochastic differential equations (SDEs) governing the dynamics of diverse engineering systems and structures (e.g., [1–3]), in many cases it can be computationally prohibitive. Therefore, there is merit in developing alternative numerical and/or analytic solution methodologies. Indicative popular approaches in stochastic engineer-

ing dynamics include moments equations and statistical linearization, stochastic averaging, discrete Chapman–Kolmogorov equation schemes, Fokker–Planck equation solution techniques, (generalized) polynomial chaos expansions, and probability density evolution methods (e.g., [4–6]).

One of the promising semi-analytical techniques relates to the concept of path integral, developed independently by Wiener [7] and by Feynman [8]. Recently, Kougioumtzoglou and co-workers developed Wiener path integral techniques for stochastic response determination and optimization of complex engineering dynamical systems. These techniques are capable of determining the joint response transition probability density function (PDF) of diverse nonlinear systems, even endowed with fractional derivative elements (e.g., [9,10]). Further, they can account for non-white and non-Gaussian stochastic process modeling [11], while it has been shown that the related computational cost can be reduced drastically by resorting to sparse representations and compressive sampling theory and tools [12]. Nevertheless, the numerical implementation of the technique is still associated with non-negligible computational cost. To address this challenge, a conceptually different solution approach has been pursued recently by the authors [13,14] by coupling the Wiener path integral formalism with a Cauchy–Schwarz inequality treatment. This has yielded a closed-form approximate expression for the system response transition PDF, whereas the computational cost has been kept at a minimal level. Note, however, that the results in [13,14] have been restricted to the class of SDEs with nonlinear drift, but constant diffusion coefficients.

In this paper, the technique developed in [13,14] is extended to account for a more general class of nonlinear SDEs, with nonlinearities appearing both in the drift and in the diffusion coefficients. Specifically, the system response PDF is derived approximately in closed form. This is done by relying on the Wiener path integral "most probable path" approximation and on the Cauchy–Schwarz inequality, in conjunction with formulating and solving an error minimization problem by utilizing the associated Fokker–Planck equation operator. Besides the mathematical merit of this generalization, its relevance to engineering dynamics applications is evident when coupled with a stochastic averaging treatment of the original second-order governing SDE. In this regard, the technique is capable

of determining approximately the response amplitude transition PDF of diverse stochastically excited nonlinear oscillators. Various nonlinear systems are considered in the numerical examples for demonstrating the accuracy and computational efficiency of the developed technique, including hysteretic systems following the Preisach versatile modeling. Comparisons with pertinent MCS data are provided as well.

2 Preliminaries

2.1 Chapman–Kolmogorov and Fokker–Planck equations

This section serves as a brief background on Markov processes, the associated Chapman–Kolmogorov (C–K), and Fokker–Planck (F–P) equations, as well as their relation to the corresponding governing SDE; see also [15,16] for some indicative standard books on the topic.

Consider a Markov stochastic process, $X_t = X(t)$, for which the C–K equation is satisfied for any $t_3 \geq t_2 \geq t_1$, i.e.,

$$p(x_3, t_3|x_1, t_1) = \int_{-\infty}^{\infty} p(x_3, t_3|x_2, t_2) p(x_2, t_2|x_1, t_1) \mathrm{d}x_2,$$
(1)

where $p(x_3, t_3|x_1, t_1)$ denotes the transition PDF of the process X_t. Further, under Lindeberg's condition, the C–K Eq. (1) leads to the well-known F–P equation governing the evolution in time of the transition PDF (e.g., see [16,17]), i.e.,

$$\frac{\partial p}{\partial t} = -\frac{\partial (\mu(x, t) \, p)}{\partial x} + \frac{1}{2} \frac{\partial^2 (\sigma(x, t)^2 p)}{\partial x^2},$$
(2)

where p is the transition PDF of the diffusion process X_t, and $\mu(\cdot, \cdot)$, $\sigma(\cdot, \cdot)$ are real-valued functions denoting the drift and diffusion coefficients, respectively, of the associated governing SDE of the form

$$\dot{x} = \mu(x, t) + \sigma(x, t)\eta(t).$$
(3)

In Eq. (3), the dot over a variable denotes differentiation with respect to time t, and $\eta(t)$ is a zero-mean and delta-correlated process of intensity one, i.e., $\mathbf{E}(\eta(t)) = 0$

and $\mathbf{E}\left((\eta(t)\eta(t-\tau))\right) = \delta_0(\tau)$, where $\delta_0(\cdot)$ is the Dirac delta function.

2.2 Wiener path integral formulation

For completeness, this section reviews the basic elements of a recently developed Wiener path integral stochastic response determination technique, which relies on the machinery of functional integrals and variational calculus; see also [11,18,19] for a more detailed presentation. The formulation of the Wiener path integral technique serves as the starting point in the ensuing analysis for deriving a closed-form expression for the system response transition PDF.

In the limit, i.e., $t_2 - t_1 = \Delta t \to 0$, the transition PDF has been shown to admit a Gaussian distribution of the form (e.g., [17])

$$p\left(x_2, t_2 | x_1, t_1\right) = \frac{\exp\left(-\frac{(x_2 - x_1 - \mu(x_1, t_1)\Delta t)^2}{2\sigma(x_1, t_1)^2 \Delta t}\right)}{\sqrt{2\pi\sigma(x_1, t_1)^2 \Delta t}}. \quad (4)$$

Note that the choice of Eq. (4) is not restrictive, and alternative non-Gaussian distributions can also be employed (e.g., [20]). Further, Eq. (4), in conjunction with the C–K Eq. (1), has been the starting point of numerical schemes (typically referred to in the literature as numerical path integral schemes) for propagating the response PDF in short time steps (e.g., [21–23]). Although these schemes have proven to be highly accurate in determining the response transition PDF, they become eventually computationally prohibitive with increasing number of dimensions. This is due to the fact that numerical computation of a multi-dimensional convolution integral is required for each and every time step.

Next, from a Wiener path integral perspective, the probability that x follows a specific path, $x(t)$, can be construed as the probability of a compound event. In particular, it can be expressed (e.g., [11,18]) as a product of probabilities by utilizing Eq. (4), i.e.,

$$P[x(t)] = \lim_{\Delta t \to 0,\ N \to \infty}$$

$$\times \frac{\exp\left(-\sum_{j=0}^{N-1} \frac{(x_{j+1} - x_j - \mu(x_j, t_j)\Delta t)^2}{2\sigma(x_j, t_j)^2 \Delta t}\right)}{\prod_{j=0}^{N-1}\sqrt{2\pi\sigma(x_j, t_j)^2 \Delta t}} \prod_{j=0}^{N-1} \mathrm{d}x_j, \quad (5)$$

where the time has been discretized into N points, Δt apart, and the path $x(t)$ is represented by its values x_j at the discrete time points t_j, for $j \in \{0, \ldots, N-1\}$. Also, $\mathrm{d}x_j$ denotes the (infinite in number) infinitesimal "gates" through which the path propagates. Loosely speaking, Eq. (5) represents the probability of the process to propagate through the infinitesimally thin tube surrounding $x(t)$. Alternatively, Eq. (5) can be written in the compact form [11,18]

$$P[x(t)]$$
$$= \exp\left(-\int_{t_i}^{t_f} \frac{(\dot{x}_j - \mu(x, t))^2}{2\sigma(x, t)^2}\mathrm{d}t\right) \prod_{t=t_i}^{t_f} \frac{\mathrm{d}x(t)}{\sqrt{2\pi\sigma(x, t)^2\mathrm{d}t}}. \quad (6)$$

Overall, the total probability that x will start from x_i at time t_i and end up at x_f at time t_f takes the form of a functional integral, which "sums up" the respective probabilities of each and every path that the process can possibly follow (e.g., see [18]). Next, denoting by $C\{x_i, t_i; x_f, t_f\}$ the set of all possible paths starting from x_i at time t_i and ending up at x_f at time t_f, the transition PDF takes the form

$$p\left(x_f, t_f | x_i, t_i\right) = \int_{C\{x_i, t_i; x_f, t_f\}} \exp\left(-\int_{t_i}^{t_f} L(x, \dot{x})\right) \mathcal{D}[x(t)]. \quad (7)$$

In Eq. (7), $L(x, \dot{x})$ represents the Lagrangian function equal to

$$L(x, \dot{x}) = \frac{1}{2}\left(\frac{\dot{x} - \mu(x, t)}{\sigma(x, t)}\right)^2, \quad (8)$$

and $\mathcal{D}[x(t)]$ is a functional measure given by

$$\mathcal{D}[x(t)] = \prod_{t=t_i}^{t_f} \frac{\mathrm{d}x(t)}{\sqrt{2\pi\sigma(x(t), t)^2\mathrm{d}t}}. \quad (9)$$

2.3 Numerical implementation and computational cost of the Wiener path integral solution technique

It is noted that the formal expression of the path integral in Eq. (7) is of little practical use as its analytical or numerical evaluation is highly challenging. Therefore,

an approximate solution approach is required. In this regard, the "most probable path" approach is employed (e.g., [11,18,19]), according to which the largest contribution to the Wiener path integral comes from the path $x_c(t)$ for which the integral in the exponential of Eq. (7) becomes as small as possible. Calculus of variations [24] dictates that this path $x_c(t)$ with fixed end points satisfies the extremality condition

$$\delta \int_{t_i}^{t_f} L(x_c, \dot{x}_c)dt = 0, \tag{10}$$

which yields the Euler–Lagrange (E–L) equation (e.g., see [9,11,19])

$$\frac{\partial L}{\partial x_c} - \frac{\partial}{\partial t}\frac{\partial L}{\partial \dot{x}_c} = 0, \tag{11}$$

to be solved in conjunction with the boundary conditions $x_c(t_i) = x_i$, $x_c(t_f) = x_f$. Once the boundary value problem (BVP) of Eq. (11) is solved and $x_c(t)$ is determined, the response transition PDF can be approximated by

$$p(x_f, t_f | x_i, t_i) \approx \Phi \exp\left(-\int_{t_i}^{t_f} L(x_c, \dot{x}_c)dt\right), \tag{12}$$

where Φ is a normalization coefficient; see also [11, 18]for a more detailed presentation.

Although the BVP of Eq. (11) can be solved analytically and yield closed-form solutions for cases of linear systems (e.g., [25,26]), it is readily seen that a numerical solution treatment is required, in general, to account for arbitrary nonlinearities in the governing Eq. (3), and consequently, in the BVP of Eq. (11). In this regard, note that, due to the fixed boundary conditions, a single point of the response transition PDF is evaluated by solving numerically one BVP of the form of Eq. (11). According to a brute-force solution scheme, and for a given time instant, an effective PDF domain is considered. Following the discretization of the domain into N points x_f, the response PDF values are determined for each point of the mesh. It is worth mentioning that for an m-dimensional version of the SDE of Eq. (3), the number of BVPs to be solved becomes N^m, i.e., the computational cost increases exponentially with the number of dimensions, and becomes prohibitive eventually. To bypass the above bottleneck, Kougioumtzoglou and co-workers have developed recently various

efficient solution techniques by resorting to appropriate response PDF expansions in conjunction with a compressive sampling treatment and group sparsity concepts. The above developments have decreased drastically the associated computational cost as compared both to a standard MCS solution approach and to the N^m BVPs required to be solved numerically by the brute-force Wiener path integral technique implementation; see also [12,27,28] for a more detailed presentation and discussion.

Nevertheless, despite the aforementioned efforts toward computational efficiency enhancement of the Wiener path integral technique, the computational cost remains non-trivial as a non-negligible number of BVPs is still required to be solved numerically for determining the response PDF. In this paper, and in the following section in particular, a conceptually different solution approach is pursued, and a closed-form approximate expression is derived for the response transition PDF. This is done in conjunction with the Wiener path integral formalism and by relying on a Cauchy–Schwarz inequality treatment, whereas the computational cost is kept at a minimal level.

3 Main results

In this section, a novel closed-form approximate expression is derived for the response transition PDF of SDEs with nonlinear drift and nonlinear diffusion coefficients of arbitrary form. In this regard, attention is directed in the ensuing analysis to a version of Eq. (3) with time-invariant nonlinear coefficients; that is,

$$\dot{x} = \mu(x) + \sigma(x)\eta(t). \tag{13}$$

Specifically, resorting to a Wiener path integral variational formulation and employing the Cauchy–Schwarz inequality yields an analytical expression for the transition PDF, whose determination requires practically zero computational cost. Further, the accuracy of the above approximation is enhanced by proposing a more versatile closed-form expression with additional "degrees of freedom," i.e., parameters to be evaluated. To this aim, an error minimization approach based on the corresponding F–P equation is formulated and solved, at the expense of some modest computational cost. The herein developed technique can be construed as an extension of earlier work by Meimaris

et al. [13,14] to account for a more general class of nonlinear SDEs, with nonlinearities appearing both in the drift and in the diffusion coefficients. Besides the mathematical merit of the aforementioned generalization, its relevance to engineering dynamics applications is significant. In particular, as shown in the numerical examples section, when coupled with a stochastic averaging treatment of the original second-order governing SDE, the technique is capable of determining approximately (at minimal, however, computational cost) the response amplitude transition PDF of diverse stochastically excited nonlinear oscillators. Systems exhibiting complex hysteretic response behaviors such as those following the Preisach versatile modeling can also be readily accounted for under the same solution framework.

3.1 Approximate closed-form transition PDF for SDEs with nonlinear drift and nonlinear diffusion coefficients

In this section, a closed-form analytical approximation is derived for the solution PDF of Eq. (13) based on a Cauchy–Schwarz inequality treatment. In this regard, the approximation can be used not only as a direct SDE response PDF estimate that requires practically zero computational effort for its determination, but also as a starting point in the optimization approach developed in the ensuing section toward enhancing the accuracy of the original, rather crude, approximation.

Specifically, following the derivation provided in "Appendix A" and taking into account Eqs. (12) and (73), an approximation for the response transition PDF of Eq. (13) is given by

$$\hat{p}(x_\mathrm{f}, t_\mathrm{f}|x_i, t_i) = \mathcal{N}(t_\mathrm{f}|x_i, t_i) \exp\left(-G(x_\mathrm{f}, t_\mathrm{f}|x_i, t_i)\right), \tag{14}$$

where

$$G(x_\mathrm{f}, t_\mathrm{f}|x_i, t_i) \\ = \frac{1}{2}\left(\frac{(\mathcal{R}(x_\mathrm{f}) - \mathcal{R}(x_i))^2}{t_\mathrm{f} - t_i} - (\mathcal{M}(x_\mathrm{f}) - \mathcal{M}(x_i))\right),$$

$$\mathcal{R}(x) = \int_{x^*}^{x} \frac{1}{\sigma(u)}\mathrm{d}u,$$

$$\mathcal{M}(x) = \int_{x^*}^{x} \frac{2\mu(u)}{\sigma(u)^2}\mathrm{d}u, \tag{15}$$

and $x^* \in \mathbb{R}$ an arbitrarily chosen point so that the integrals of Eq. (15) are well defined. Further, the normalization constant $\mathcal{N}$ in Eq. (14) is determined as

$$\mathcal{N}(t_\mathrm{f}|x_i, t_i) = \left(\int_{\mathcal{D}} \exp\left(-G(z, t_\mathrm{f}|x_i, t_i)\right)\mathrm{d}z\right)^{-1}, \tag{16}$$

where $\mathcal{D}$ denotes the domain of integration, accounting for any restrictions that $\mathcal{M}(\cdot)$ and $\mathcal{R}(\cdot)$ may impose. Clearly, further manipulation of the closed-form expression of Eqs. (14)–(15) depends on the availability of analytical expressions for the antiderivatives $\mathcal{M}(\cdot)$ and $\mathcal{R}(\cdot)$, which in turn depends on the specific nonlinearity form under consideration.

It can be readily seen that $\hat{p}(\cdot)$ in Eq. (14) can be directly used as an analytical approximation of the response process transition PDF without resorting to the numerical solution of the E–L Eq. (11). Note that the closed-form expression of Eq. (14), which requires essentially zero computational cost for its evaluation, can be construed as a generalization of the expression derived in [13] to account for nonlinearities both in the drift and in the diffusion coefficients of the governing stochastic differential Eq. (13).

3.2 Enhanced accuracy via an error minimization scheme

As demonstrated in [13] for the case of SDEs with nonlinear drift but constant diffusion coefficients, although the approximation of Eq. (14) is capable, in general, of capturing the salient features of the solution PDF, in many cases the degree of accuracy exhibited can be inadequate. To address this limitation, a more general form of the PDF was proposed in [14], by incorporating two additional "degrees of freedom," i.e., parameters to be determined based on an appropriate optimization scheme. Similarly to [14], and to address the herein considered more challenging case of SDEs with nonlinearities both in the drift and in the diffusion coefficients, a more general form than Eq. (14) is proposed for the transition PDF, that is,

$$\hat{p}_{(k,n)}(x_\mathrm{f}, t_\mathrm{f}|x_i, t_i) \\ = \mathcal{N}_{(k,n)}(t_\mathrm{f}|x_i, t_i) \exp\left(-G_{(k,n)}(x_\mathrm{f}, t_\mathrm{f}|x_i, t_i)\right), \tag{17}$$

where

$$G_{(k,n)}(x_{\mathrm{f}}, t_{\mathrm{f}}|x_i, t_i)$$
$$= \frac{1}{2}\left(k\frac{(\mathcal{R}(x_{\mathrm{f}}) - \mathcal{R}(x_i))^2}{t_{\mathrm{f}} - t_i} - n\left(\mathcal{M}(x_{\mathrm{f}}) - \mathcal{M}(x_i)\right)\right),$$
(18)

and the normalization constant $\mathcal{N}$ in Eq. (17) is given by

$$\mathcal{N}_{(k,n)}(t_{\mathrm{f}}|x_i, t_i) = \left(\int_{\mathcal{D}} \exp\left(-G_{(k,n)}(z, t_{\mathrm{f}}|x_i, t_i)\right)\mathrm{d}z\right)^{-1}.$$
(19)

Note that the additional parameters k and n render the rather crude PDF approximation of Eq. (14) more versatile in capturing diverse response behaviors. In particular, the parameter k relates to optimizing and "tightening" the Cauchy–Schwarz inequality of Eq. (72), whereas the parameter n refers to the overall accuracy of the Wiener path integral approximation of Eq. (12). This generalized PDF form is anticipated to enhance the accuracy exhibited by Eq. (14), at the expense, however, of some modest computational cost related to the determination of k and n.

Specifically, to determine the parameters k and n in Eq. (17), for a given norm ($\|\cdot\|_q$), the error quantity $\|\hat{p}_{(k,n)} - p^*\|_q$ is sought to be minimized, where p^* denotes the exact solution PDF. However, since p^* is unknown, an error minimization scheme based on the F–P equation operator is adopted in the ensuing analysis (see also [14]). In this regard, the exact transition PDF p^* for the SDE of Eq. (13) is given as the solution of the F–P equation [Eq. (2)] associated with Eq. (13), i.e.,

$$\frac{\partial p^*(x, t)}{\partial t} = -\frac{\partial\left(\mu(x)\,p^*(x, t)\right)}{\partial x}$$
$$+ \frac{1}{2}\frac{\partial^2\left(\sigma(x)^2 p^*(x, t)\right)}{\partial x^2}.$$
(20)

Next, denoting the F–P operator as

$$\mathcal{L}_{\mathrm{FP}}[p(x, t)] = \frac{\partial p(x, t)}{\partial t} + \frac{\partial\left(\mu(x)\,p(x, t)\right)}{\partial x}$$
$$- \frac{1}{2}\frac{\partial^2\left(\sigma(x)^2 p(x, t)\right)}{\partial x^2},$$
(21)

and taking into account that $\mathcal{L}_{\mathrm{FP}}[p^*] = 0$, the error is defined as

$$\mathrm{err}_q = \|\mathcal{L}_{\mathrm{FP}}[\hat{p}_{(k,n)} - p^*]\|_q$$
$$= \|\mathcal{L}_{\mathrm{FP}}[\hat{p}_{(k,n)}] - \mathcal{L}_{\mathrm{FP}}[p^*]\|_q$$
$$= \|\mathcal{L}_{\mathrm{FP}}[\hat{p}_{(k,n)}]\|_q.$$
(22)

Due to the analytical form of $\hat{p}_{(k,n)}$ in Eq. (17), the error quantity $\mathrm{err}_q = \|\mathcal{L}_{\mathrm{FP}}[\hat{p}_{(k,n)}]\|_q$ in Eq. (22) can be expressed explicitly as a function of k and n; see also [14]. Further, for a chosen q-norm and final time t_{f}, the values of k, n are numerically evaluated by solving the optimization problem

$$\hat{z}_q = \left(\hat{k}, \hat{n}\right)_q = \arg\min_{k, n \in \mathbb{R}} \|\mathcal{L}_{\mathrm{FP}}[\hat{p}_{(k,n)}(\cdot, t_{\mathrm{f}})]\|_q, \quad (23)$$

and thus, the approximate response PDF of Eq. (17) is determined.

4 Response analysis of stochastically excited nonlinear/hysteretic oscillators

In this section, it is shown that the developed solution technique in Sect. 3 can be readily coupled with a stochastic averaging treatment of the second-order SDEs governing the dynamics of diverse stochastically excited nonlinear/hysteretic oscillators for determining the response transition PDF in a computationally efficient manner. Concisely, the main aspects of stochastic averaging (e.g., [30,31]) relate to a Markovian approximation of an appropriately chosen amplitude of the system response, as well as to a dimension reduction of the original two-dimensional problem to an one-dimensional problem. In particular, the original second-order SDE is cast into a first-order SDE of the form of Eq. (13), and thus, the technique developed in Sect. 3 can be applied in a straightforward manner.

In this regard, consider a nonlinear single-degree-of-freedom oscillator whose motion is governed by

$$\ddot{y} + \beta_0\dot{y} + g(t, y, \dot{y}) = v(t), \quad (24)$$

where $v(t)$ is a white noise process, i.e., $\mathbf{E}(v(t)) = 0$ and $\mathbf{E}(v(t_1)v(t_2)) = 2\pi S_0\delta_0(t_1 - t_2)$, $g(\cdot)$ is the restoring force which can be either hysteretic or depend only on the instantaneous values of y and $\dot{y}$, β_0 is a linear damping coefficient so that $\beta_0 = 2\zeta_0\omega_0$; ζ_0 is

the ratio of critical damping, and ω_0 is the natural frequency corresponding to the linear oscillator (i.e., $g(t, y, \dot{y}) = \omega_0^2 y$).

Next, adopting the assumption of light damping (e.g., $\zeta_0 \ll 1$), it can be argued that the oscillator of Eq. (24) exhibits a pseudo-harmonic response behavior described by the equations (e.g., [32])

$$y(t) = x \cos(\omega(x)t + \phi), \tag{25}$$

and

$$\dot{y}(t) = -x\omega(x) \sin(\omega(x)t + \phi). \tag{26}$$

Manipulating Eqs. (25) and (26), the response amplitude x and the response phase ϕ are given by

$$x(t) = \sqrt{y(t)^2 + \frac{\dot{y}(t)^2}{\omega(x)^2}}, \tag{27}$$

and

$$\phi(t) = -\omega(x)t - \tan^{-1}\left(\frac{\dot{y}(t)}{y(t)\omega(x)}\right), \tag{28}$$

respectively. These are considered to be slowly varying functions with respect to time, and approximately constant over one cycle of oscillation; see also [31,32]. In Eqs. (25) and (26), the equivalent natural frequency $\omega(x)$, to be determined in the following, is approximated as a function of the response amplitude x to account for the effect of nonlinearities in the original system of Eq. (24). Next, a statistical linearization treatment (e.g., [4,32]) yields an equivalent to Eq. (24) oscillator of the form

$$\ddot{y} + \beta(x)\dot{y} + \omega(x)^2 y = v(t), \tag{29}$$

where

$$\beta(x) = \beta_0 - \frac{\frac{1}{\pi}\int_0^{2\pi} \sin(\psi)g(t, x\cos(\psi), -\omega x \sin(\psi))d\psi}{x\omega(x)}, \tag{30}$$

and

$$\omega(x)^2 = \frac{\frac{1}{\pi}\int_0^{2\pi} \cos(\psi)g(t, x\cos(\psi), -\omega x \sin(\psi))d\psi}{x}. \tag{31}$$

Further, resorting to a stochastic averaging treatment (e.g., [32]), the response amplitude x can be decoupled from the response phase ϕ, yielding a first-order stochastic differential equation for x in the form

$$\dot{x} = -\frac{1}{2}\beta(x)x + \frac{\pi S_0}{2x\omega(x)^2} + \frac{\sqrt{\pi S_0}}{\omega(x)}\eta(t). \tag{32}$$

It can be readily seen that Eq. (32) is an SDE of the form of Eq. (13) with drift μ and diffusion σ coefficients given by

$$\mu(x) = -\frac{1}{2}\beta(x)x + \frac{\pi S_0}{2x\omega(x)^2}, \tag{33}$$

and

$$\sigma(x) = \sqrt{\frac{\pi S_0}{\omega(x)^2}}, \tag{34}$$

respectively. Thus, the herein developed solution technique can be applied in a straightforward manner for determining the stochastic response of a wide range of nonlinear/hysteretic oscillators.

5 Numerical examples

In this section, the hardening Duffing and hysteretic Preisach nonlinear oscillators are considered for assessing the reliability of the herein developed technique. In this regard, a standard interior point method [33,34] using Matlab's *fmincon* built-in function is employed for solving numerically the optimization problem of Eq. (23) in conjunction with the $\|\cdot\|_2$ norm. To this aim, the basic approximation of Eq. (14) with $(k, n) = (1, 1)$ serves as a natural choice for the starting point of the optimization algorithm. In all cases, the algorithm converged in no more than 55 iterations, which translates into a small fraction of a second from a computational cost perspective. The response transition PDF obtained by the closed-form expression of Eq. (32) is compared with pertinent MCS-based PDF estimates produced by numerically integrating the original equation of motion, Eq. (24) (100,000 realizations). A standard computer with 16 GB RAM, Inter(R) Core(TM) i7-6700 CPU @3.40 GHz, is used for the numerical implementations.

5.1 Duffing nonlinear oscillator

In the case of a Duffing oscillator, the equation of motion is governed by Eq. (24), with

$$g(t, y, \dot{y}) = \omega_0^2 \left(y + \alpha y^3 \right),$$ (35)

and α is a parameter controlling the nonlinearity magnitude. Next, utilizing Eqs. (30) and (31) yields

$$\beta(x) = \beta_0,$$ (36)

and

$$\omega(x)^2 = \omega_0^2 \left(1 + \frac{3}{4} \alpha x^2 \right).$$ (37)

Thus, by employing Eqs. (36–37), the drift and diffusion coefficients of Eqs. (33–34) become

$$\mu(x) = -\frac{1}{2} \beta_0 x + \frac{\pi S_0}{2 x \omega_0^2 \left(1 + \frac{3}{4} \alpha x^2 \right)},$$ (38)

and

$$\sigma(x) = \sqrt{\frac{\pi S_0}{\omega_0^2 \left(1 + \frac{3}{4} \alpha x^2 \right)}},$$ (39)

respectively.

Further, the antiderivatives $R(\cdot)$ and $M(\cdot)$ take the form

$$\sqrt{\pi S_0} \mathcal{R}(x)$$
$$= \omega_0 \left(\frac{\sinh^{-1} \left(\sqrt{\frac{3}{4} \alpha} \, x \right)}{\sqrt{3\alpha}} + \frac{x \sqrt{\frac{3}{4} \alpha \, x^2 + 1}}{2} \right),$$ (40)

where $\sinh^{-1}(x) = \ln(x + \sqrt{1 + x^2})$ and

$$\mathcal{M}(x) = \ln(x) - \frac{\beta_0 \omega_0^2}{2\pi S_0} x^2 - \frac{3 \beta_0 \omega_0^2 \alpha}{16 \pi S_0} x^4,$$ (41)

respectively. Thus, the nonlinear Duffing oscillator response amplitude PDF has been expressed in closed form according to Eq. (17).

In the following numerical example, the parameter values $\omega_0 = 1$, $\zeta_0 = 0.01$, $S_0 = \frac{6}{\pi} \zeta_0$ and the initial

conditions $y(t_i = 0) = 1$, $\dot{y}(t_i = 0) = 0$ are considered. Next, minimizing the error as defined in Eq. (23) for a given time instant yields the values for k and n. Two time instants are considered, the first ($t_f = 2s$) corresponding to the transient phase of the response behavior, and the second ($t_f = 50s$) corresponding effectively to the stationary regime. For $t_f = 2s$ and $t_f = 50s$, the respective objective functions of Eq. (23) are plotted in Figs. 1 and 2, respectively, for nonlinearity magnitude $\alpha = 1$. The computed values of k and n are shown in Table 1 together with the corresponding iterations numbers and CPU times of the optimization algorithm. In Fig. 3, both the basic $\hat{p}_{(1,1)}$ and the enhanced $\hat{p}_{(k,n)}$ approximations are plotted for the above two time instants and compared with pertinent MCS-based PDF estimates. It is seen that for early time instants ($t_f = 2s$) $\hat{p}_{(1,1)}$ manages to capture the basic features of the response amplitude PDF and yields comparable accuracy to $\hat{p}_{(k,n)}$. However, the superior performance of $\hat{p}_{(k,n)}$ over $\hat{p}_{(1,1)}$ becomes evident at $t_f = 50s$ (stationary phase). In fact, comparisons both with MCS data and with the available stationary analytical solution of the F–P Eq. (20) (e.g., [31]), i.e.,
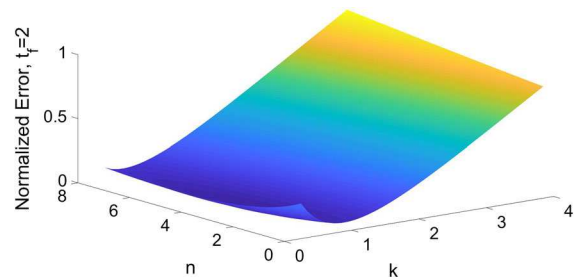

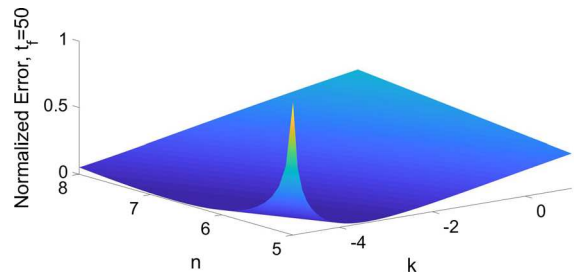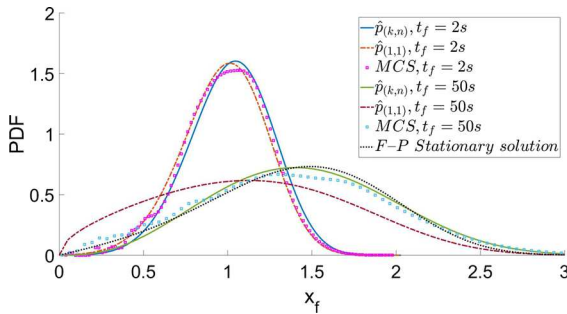**Fig. 1** Objective function of Eq. (23) for a Duffing oscillator with $\alpha = 1$ at $t_f = 2$

Fig. 2 Objective function of Eq. (23) for a Duffing oscillator with $\alpha = 1$ at $t_f = 50$

Table 1 Computed k and n values for various final time instants t_f and starting point $(1, 1)$ for a Duffing oscillator with $\alpha = 1$

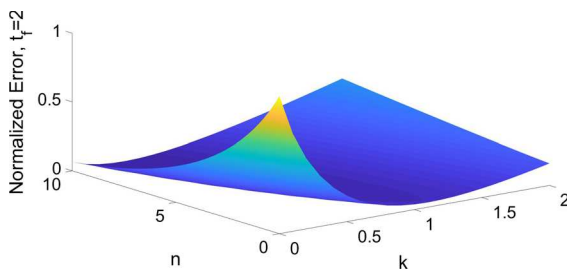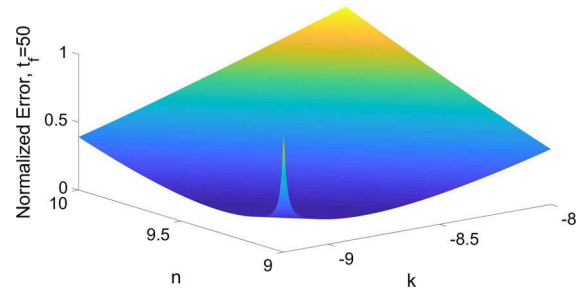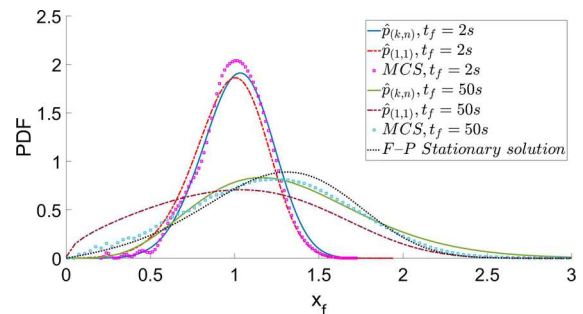|	k	n	Iterations	CPU time
$t_f = 2$	0.7949	3.5083	39	0.048
$t_f = 50$ (stationary)	-4.4646	6.1254	54	0.135

Fig. 3 Approximate response PDFs $\hat{p}_{(k,n)}$ and $\hat{p} = \hat{p}_{(1,1)}$ for various time instants t_f for a Duffing oscillator with $\alpha = 1$; comparisons with MCS-based PDF estimates (100,000 realizations) and with existing analytical stationary PDF expressions

$$p(x_f) = \frac{x_f + \alpha x_f^3}{A^2} \exp\left(-\frac{\left(\frac{1}{2}x_f^2 + \frac{\alpha}{4}x_f^4\right)}{A^2}\right), \qquad (42)$$

where

$$A^2 = \frac{\pi S_0}{2\zeta_0 \omega_0^3}, \qquad (43)$$

indicate a high accuracy degree exhibited by the approximate PDF $\hat{p}_{(k,n)}$. Similar results are shown in Figs. 4, 5 and 6 and Table 2 for nonlinearity magnitude $\alpha = 2$.

Fig. 4 Objective function of Eq. (23) for a Duffing oscillator with $\alpha = 2$ at $t_f = 2$

Fig. 5 Objective function of Eq. (23) for a Duffing oscillator with $\alpha = 2$ at $t_f = 50$

Fig. 6 Approximate response PDFs $\hat{p}_{(k,n)}$ and $\hat{p} = \hat{p}_{(1,1)}$ for various time instants t_f for a Duffing oscillator with $\alpha = 2$; comparisons with MCS-based PDF estimates (100,000 realizations) and with existing analytical stationary PDF expressions

Table 2 Computed k and n values for various final time instants t_f and starting point $(1, 1)$ for a Duffing oscillator with $\alpha = 2$

	k	n	Iterations	CPU time
$t_f = 2$	0.4525	8.6760	42	0.191
$t_f = 50$ (stationary)	-9.0246	9.1555	51	0.157

5.2 Preisach hysteretic oscillator

In the context of engineering dynamics, hysteresis can be construed as a memory-dependent relationship, which describes the dependence of the system restoring force $g(t, y, \dot{y})$ on the time history of the system response. A mathematical description of various hysteretic models can be found in [35,36]. Recently, the Preisach hysteretic model has been adopted to describe the response behavior of smart materials, such as shape-memory alloys [37,38]. The model is significantly versatile in representing diverse hysteretic patterns, and even capable of capturing minor loops present in many physical phenomena. A detailed pre-

sentation of the Preisach formalism is given in [39], while indicative contributions toward determining the stochastic response and assessing the reliability of systems endowed with Preisach elements can be found in [32,40–46].

Following the notation adopted in [41], the Preisach hysteretic restoring force, $f(t)$, is given by

$$f(t) = \iint_{a \geq b} \mu(a, b)\gamma(x, t)\mathrm{d}a\, \mathrm{d}b, \tag{44}$$

where $\gamma(x, t)$ is a relay operator or hysteron. Although the model of Eq. (44) can represent various hysteretic behaviors by appropriately identifying the weight function $\mu(a, b)$ (see also [37]), the one corresponding to the Iwan–Jenkins model is utilized in the following. Specifically, the equation of motion [Eq. (24)] becomes

$$\ddot{y} + \beta_0 \dot{y} + \bar{\omega}^2 y + f_{\mathrm{H}}(t) = v(t), \tag{45}$$

where

$$\bar{\omega}^2 = \omega_0^2 + \omega_j^2 = \omega_j^2(\varphi + 1) = k_j(1 + \varphi), \tag{46}$$

i.e., $k_j = \omega_j^2$ and $\varphi = \frac{\omega_0^2}{\omega_j^2}$. In Eqs. (45–46), it is seen that the Preisach restoring force is divided into a linear part and a nonlinear one monitoring the memory of the system, while φ quantifies the contribution of the Preisach linear part as compared to the stiffness of the corresponding linear oscillator. Next, introducing the parameter

$$\psi = \frac{\bar{\omega}^2}{f_y^\star}, \tag{47}$$

Equation (45) can be cast in the form

$$\ddot{y} + \beta_0 \dot{y} + \bar{\omega}^2 (y + \psi d_{\mathrm{H}}(t)) = v(t), \tag{48}$$

where $d_{\mathrm{H}}(t)$ denotes the scaled hysteretic restoring force. Further, for the case

$$\frac{f_{y,\mathrm{max}} - f_{y,\mathrm{min}}}{f_{y,\mathrm{max}} + f_{y,\mathrm{min}}} = 1, \tag{49}$$

where f_y is the yielding force, utilizing Eqs. (30) and (31) yields

$$\beta(x) = \beta_0 + \frac{\psi \bar{\omega}^2 x}{3\pi (1 + \varphi)^2 \sqrt{\bar{\omega}^2 - \frac{\psi \bar{\omega}^2 x}{4(1+\varphi)^2}}}, \tag{50}$$

and

$$\omega(x)^2 = \bar{\omega}^2 - \frac{\psi \bar{\omega}^2 x}{4 (1 + \varphi)^2}. \tag{51}$$

Thus, by employing Eqs. (50–51), the drift and diffusion coefficients of Eqs. (33–34) become

$$\mu(x) = -\frac{\beta_0}{2} x - \frac{\psi \bar{\omega}^2 x^2}{6\pi (1 + \varphi)^2 \sqrt{\bar{\omega}^2 - \frac{\psi \bar{\omega}^2 x}{4(1+\varphi)^2}}} + \frac{\pi S_0}{2x \left(\bar{\omega}^2 - \frac{\psi \bar{\omega}^2 x}{4(1+\varphi)^2}\right)}, \tag{52}$$

and

$$\sigma(x) = \sqrt{\frac{\pi S_0}{\bar{\omega}^2 - \frac{\bar{\omega}^2 \psi x}{4(\varphi+1)^2}}}, \tag{53}$$

respectively. The reader is also directed to [41,43] for more details on stochastic averaging of Preisach oscillators.

Further, the antiderivatives $R(\cdot)$ and $M(\cdot)$ take the form

$$\mathcal{R}(x) = -\frac{\bar{\omega}^2 A_{\varphi,\psi}(x)^2 \sqrt{\frac{\pi S_0 (\varphi+1)^2}{\bar{\omega}^2 A_{\varphi,\psi}(x)}}}{3 \pi S_0 \psi (\varphi + 1)^2}, \tag{54}$$

and

$$\mathcal{M}(x) = \log(x)$$
$$+ \frac{\frac{\beta_0 \bar{\omega}^6 A_{\varphi,\psi}(x)^3}{24} + \frac{\beta_0 \bar{\omega}^6 \psi x A_{\varphi,\psi}(x)^2}{8}}{\pi S_0 \bar{\omega}^4 \psi^2 (\varphi + 1)^2}$$
$$+ \frac{\frac{8 \bar{\omega}^7 A_{\varphi,\psi}(x)^{7/2}}{315} + \frac{4 \bar{\omega}^7 \psi x A_{\varphi,\psi}(x)^{5/2}}{45} + \frac{\bar{\omega}^7 \psi^2 x^2 A_{\varphi,\psi}(x)^{3/2}}{9}}{\pi S_0 \bar{\omega}^4 \psi^2 \pi (\varphi + 1)^3}, \tag{55}$$

respectively, where $A_{\varphi,\psi}(x) = \left(4 \varphi^2 + 8 \varphi - \psi x + 4\right)$. Thus, the nonlinear hysteretic Preisach oscillator response amplitude PDF has been expressed in closed form according to Eq. (17).

In the numerical example, the parameter values $\bar{\omega} = 1, \zeta_0 = 0.01, S_0 = \frac{2}{\pi}\zeta_0$ with $\psi = 1$ are used together with the initial conditions $y(t_i = 0) = 1$, $\dot{y}(t_i = 0) = 0$. Next, minimizing the error in Eq. (23) for a given time instant yields the values for k and n. In a similar manner as in Sect. 5.1, two time instants are considered, the first ($t_f = 5s$) corresponding to the transient phase of the response behavior, and the second ($t_f = 50s$) corresponding effectively to the stationary regime. For $t_f = 5s$ and $t_f = 50s$ the objective functions of Eq. (23) are plotted in Figs. 7 and 8, respectively, for nonlinearity magnitude $\varphi = 1$. The computed values of k and n are shown in Table 3 together with the corresponding iterations numbers and CPU times of the optimization algorithm. In Fig. 9, both the basic $\hat{p}_{(1,1)}$ and the enhanced $\hat{p}_{(k,n)}$ approximations are plotted for the above two time instants and compared
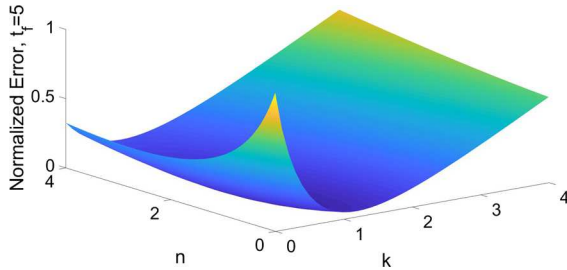

Fig. 7 Objective function of Eq. (23) for a Preisach oscillator with $\varphi = 1$ at $t_f = 5$
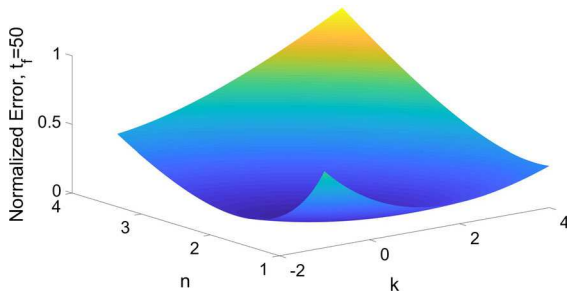

Fig. 8 Objective function of Eq. (23) for a Preisach oscillator with $\varphi = 1$ at $t_f = 50$

Table 3 Computed k and n values for various final time instants t_f and starting point (1, 1) for a Preisach oscillator with $\varphi = 1$

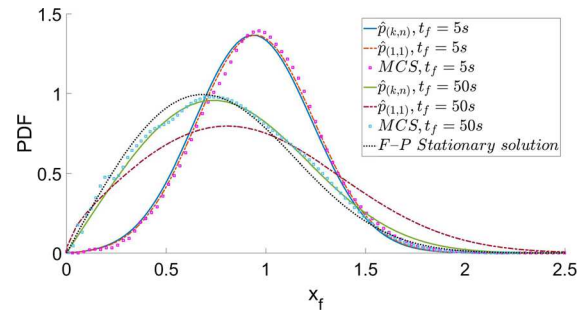|	k	n	Iterations	CPU time
$t_f = 5$	0.9440	1.2226	33	0.023
$t_f = 50$ (stationary)	0.1928	1.9673	48	0.053

Fig. 9 Approximate response PDFs $\hat{p}_{(k,n)}$ and $\hat{p} = \hat{p}_{(1,1)}$ for various time instants t_f for a Preisach oscillator with $\varphi = 1$; comparisons with MCS-based PDF estimates (100,000 realizations) and with existing analytical stationary PDF expressions

with pertinent MCS-based PDF estimates. It is seen that for early time instants ($t_f = 5s$) $\hat{p}_{(1,1)}$ manages to capture the salient features of the response amplitude PDF and appears to be almost indistinguishable from $\hat{p}_{(k,n)}$. This is also seen by observing the values for k and n in Table 3, which are relatively close to 1. Further, the enhanced accuracy of $\hat{p}_{(k,n)}$ as compared to $\hat{p}_{(1,1)}$ becomes evident at $t_f = 50s$ (stationary phase). In fact, comparisons both with MCS data and with the available stationary analytical solution of the F–P Eq. (20) (e.g., [41]), i.e.,

$$p(x_f) = C(\lambda)x_f \left(\frac{2\zeta_0}{1 - \lambda x_f}\right)^{-1/2}$$
$$\exp\left(-\frac{x_f^2}{2} + \frac{\lambda x_f^3}{12}\right.$$
$$\left. + \frac{(128 + 48\lambda x_f + 15\lambda^2 x_f^2)(4 - \lambda x_f)^{3/2}}{630\pi\zeta_0\lambda^2}\right), \tag{56}$$

where

$$\lambda = \frac{\psi}{(1 + \phi)^2}, \tag{57}$$

and $C(\lambda)$ is a normalization coefficient, indicate a satisfactory level of agreement. Similar results are shown in Figs. 10, 11 and 12 and Table 4 for nonlinearity magnitude $\varphi = 2$.
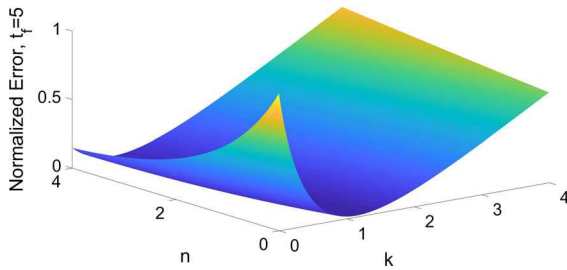
Fig. 10 Objective function of Eq. (23) for a Preisach oscillator with $\varphi = 2$ at $t_f = 5$
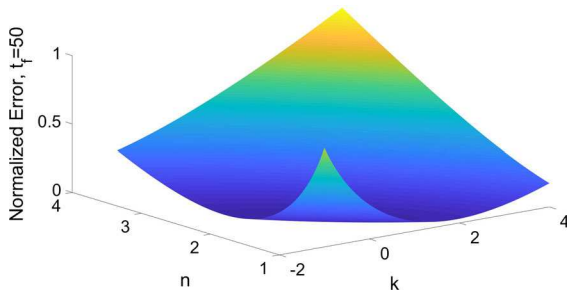

Fig. 11 Objective function of Eq. (23) for a Preisach oscillator with $\varphi = 2$ at $t_f = 50$
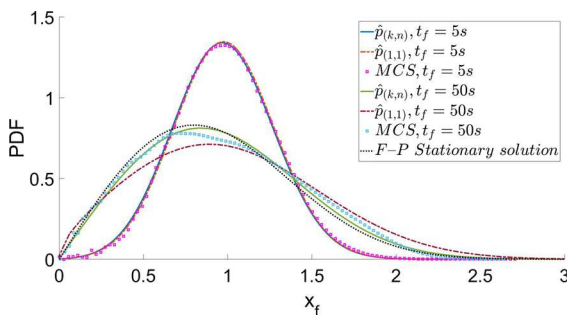

Fig. 12 Approximate response PDFs $\hat{p}_{(k,n)}$ and $\hat{p} = \hat{p}_{(1,1)}$ for various time instants t_f for a Preisach oscillator with $\varphi = 2$; comparisons with MCS-based PDF estimates (100,000 realizations) and with existing analytical stationary PDF expressions

Table 4 Computed k and n values for various final time instants t_f and starting point $(1, 1)$ for a Preisach oscillator with $\varphi = 2$

	k	n	Iterations	CPU time
$t_f = 5$	0.9358	1.3059	27	0.042
$t_f = 50$ (stationary)	0.2215	1.9201	51	0.051

6 Concluding remarks

In this paper, an approximate analytical technique has been developed for determining, in closed form and at minimal computational cost, the transition PDF of a wide range of nonlinear first-order SDEs. This has been done by relying on the Wiener path integral "most probable path" approximation and on the Cauchy–Schwarz inequality, in conjunction with formulating and solving an error minimization problem by utilizing the associated Fokker–Planck equation operator. The technique can be construed as an extension of the results in [13,14] to account for a more general class of SDEs with nonlinearities both in the drift and in the diffusion coefficients. Besides the mathematical merit of this generalization, the technique can serve also as a benchmark for assessing the performance of alternative, more computationally demanding, stochastic dynamics numerical methodologies. Further, its relevance to engineering dynamics applications has been demonstrated by determining approximately the response amplitude transition PDF of diverse stochastically excited nonlinear oscillators, including hysteretic systems following the Preisach versatile modeling. Comparisons with pertinent MCS data have demonstrated a satisfactory accuracy degree.

Compliance with ethical standards

Conflict of interest The authors have declared that no conflict of interest exists, and this paper has been approved by all authors for publication.

Appendix A: Derivation of Eq. (14)

Employing the Wiener path integral approximate solution technique and substituting the associated Lagrangian function of Eq. (8) into the E–L Eq. (11) yields

$$\frac{\ddot{x}_c - \frac{\partial \mu(x_c)}{\partial x_c}\dot{x}_c}{\sigma(x_c)^2} - 2\frac{(\dot{x}_c - \mu(x_c))\frac{\partial \sigma(x_c)}{\partial x_c}\dot{x}_c}{\sigma(x_c)^3}$$
$$= -\frac{(\dot{x}_c - \mu(x_c))\frac{\partial \mu(x_c)}{\partial x_c}}{\sigma(x_c)^2} - \frac{(\dot{x}_c - \mu(x_c))^2\frac{\partial \sigma(x_c)}{\partial x_c}}{\sigma(x_c)^3}. \tag{58}$$

Equation (58) can be further manipulated into

$$\ddot{x}_c - \mu(x_c)\frac{\partial \mu(x_c)}{\partial x_c} = \frac{\frac{\partial \sigma(x_c)}{\partial x_c}}{\sigma(x_c)}\left(\dot{x}_c^2 - \mu(x_c)^2\right), \tag{59}$$

in conjunction with the boundary conditions $x_c(t_i) = x_i$, $x_c(t_f) = x_f$. Equivalently, Eq. (59) can be cast into the form

$$\ddot{x}_c - \frac{\frac{\partial \sigma(x_c)}{\partial x_c}}{\sigma(x_c)}\dot{x}_c^2 = \mu(x_c)\frac{\partial \mu(x_c)}{\partial x_c} - \frac{\mu(x_c)^2\frac{\partial \sigma(x_c)}{\partial x_c}}{\sigma(x_c)}$$
$$= \frac{\mu(x_c)}{\sigma(x_c)}\left(\sigma(x_c)\frac{\partial \mu(x_c)}{\partial x_c} - \mu(x_c)\frac{\partial \sigma(x_c)}{\partial x_c}\right), \tag{60}$$

and multiplying both sides by $\frac{2\dot{x}_c}{\sigma(x_c)^2}$ yields

$$\frac{2\dot{x}_c\ddot{x}_c}{\sigma(x_c)^2} - \frac{2\frac{\partial \sigma(x_c)}{\partial x_c}}{\sigma(x_c)^3}\dot{x}_c^3$$
$$= 2\frac{\mu(x_c)}{\sigma(x_c)}\left(\frac{\sigma(x_c)\frac{\partial \mu(x_c)}{\partial x_c} - \mu(x_c)\frac{\partial \sigma(x_c)}{\partial x_c}}{\sigma(x_c)^2}\right)\dot{x}_c. \tag{61}$$

Next, taking into account that

$$\frac{\partial}{\partial x_c}\left(\left(\frac{\mu(x_c)}{\sigma(x_c)}\right)^2\right)$$
$$= 2\frac{\mu(x_c)}{\sigma(x_c)}\left(\frac{\sigma(x_c)\frac{\partial \mu(x_c)}{\partial x_c} - \mu(x_c)\frac{\partial \sigma(x_c)}{\partial x_c}}{\sigma(x_c)^2}\right), \tag{62}$$

in conjunction with the chain rule of differentiation, i.e., $\frac{d}{dt}\left(\left(\frac{\mu(x_c)}{\sigma(x_c)}\right)^2\right) = \frac{\partial}{\partial x_c}\left(\left(\frac{\mu(x_c)}{\sigma(x_c)}\right)^2\right)\dot{x}_c$, Eq. (61) becomes

$$\frac{2\dot{x}_c\ddot{x}_c}{\sigma(x_c)^2} - \frac{2\frac{\partial \sigma(x_c)}{\partial x_c}}{\sigma(x_c)^3}\dot{x}_c^3 = \frac{d}{dt}\left(\left(\frac{\mu(x_c)}{\sigma(x_c)}\right)^2\right). \tag{63}$$

Further, it can be readily verified that

$$\frac{d}{dt}\left(\frac{\dot{x}_c^2}{\sigma(x_c)^2}\right) = \frac{2\dot{x}_c\ddot{x}_c}{\sigma(x_c)^2} - \frac{2\frac{\partial \sigma(x_c)}{\partial x_c}}{\sigma(x_c)^3}\dot{x}_c^3. \tag{64}$$

Utilizing Eq. (64), Eq. (63) becomes

$$\frac{d}{dt}\left(\frac{\dot{x}_c^2}{\sigma(x_c)^2}\right) = \frac{d}{dt}\left(\left(\frac{\mu(x_c)}{\sigma(x_c)}\right)^2\right), \tag{65}$$

or, alternatively,

$$\frac{\dot{x}_c^2}{\sigma(x_c)^2} = \left(\frac{\mu(x_c)}{\sigma(x_c)}\right)^2 + b, \tag{66}$$

where b is a constant, dependent on the boundary conditions, i.e., $x_c(t_i) = x_i$, $x_c(t_f) = x_f$. Considering next Eq. (8), and expanding, leads to

$$L(x_c, \dot{x}_c) = \frac{1}{2}\left(\frac{\dot{x}_c^2 - 2\dot{x}_c\mu(x_c) + \mu(x_c)^2}{\sigma(x_c)^2}\right), \tag{67}$$

whereas substituting Eq. (66) into Eq. (67) yields

$$L(x_c, \dot{x}_c) = \frac{1}{2}\left(\frac{2\dot{x}_c^2 - 2\dot{x}_c\mu(x_c)}{\sigma(x_c)^2} - b\right). \tag{68}$$

Next, integrating Eq. (68) leads to

$$\int_{t_i}^{t_f} L(x_c, \dot{x}_c)dt$$
$$= \frac{1}{2}\left(2\int_{t_i}^{t_f}\frac{\dot{x}_c^2}{\sigma(x_c)^2}dt - \int_{t_i}^{t_f}\frac{2\dot{x}_c\mu(x_c)}{\sigma(x_c)^2}dt \right.$$
$$\left. - b\left(t_f - t_i\right)\right). \tag{69}$$

Furthermore, for arbitrary functions $f(\cdot)$, $g(\cdot)$, the Cauchy–Schwarz inequality (e.g., [29]) states that

$$\left(\int_a^b f(t)g(t)dt\right)^2 \leq \int_a^b f(t)^2dt\int_a^b g(t)^2dt. \tag{70}$$

Clearly, setting $f \equiv 1$ yields the special case

$$\int_a^b g(t)^2dt \geq \frac{1}{b-a}\left(\int_a^b g(t)dt\right)^2. \tag{71}$$

Next, denoting by $\mathcal{M}(\cdot)$ an antiderivative of $\frac{2\mu(\cdot)}{\sigma(\cdot)^2}$ and by $\mathcal{R}(\cdot)$ an antiderivative of $\frac{1}{\sigma(\cdot)}$, and applying Eq. (71) to the term $2\int_{t_i}^{t_f} \frac{\dot{x}_c^2}{\sigma(x_c)^2}dt$ in Eq. (69) yields

$$
\begin{aligned}
2\int_{t_i}^{t_f} \frac{\dot{x}_c^2}{\sigma(x_c)^2}dt &\geq \int_{t_i}^{t_f} \frac{\dot{x}_c^2}{\sigma(x_c)^2}dt \\
&\geq \frac{\left(\int_{t_i}^{t_f} \frac{\dot{x}_c}{\sigma(x_c)}dt\right)^2}{t_f - t_i} \\
&= \frac{(\mathcal{R}(x_f) - \mathcal{R}(x_i))^2}{t_f - t_i}.
\end{aligned}
\tag{72}
$$

Considering Eq. (72), Eq. (69) becomes

$$
\begin{aligned}
\int_{t_i}^{t_f} L(x_c, \dot{x}_c)dt &\geq -\frac{b(t_f - t_i)}{2} \\
&+ \frac{1}{2}\left(\frac{(\mathcal{R}(x_f) - \mathcal{R}(x_i))^2}{t_f - t_i} - (\mathcal{M}(x_f) - \mathcal{M}(x_i))\right).
\end{aligned}
\tag{73}
$$

Thus, taking into account Eqs. (12) and (73) an approximation for the response transition PDF of Eq. (13) is given by

$$
\hat{p}(x_f, t_f | x_i, t_i) = \mathcal{N}(t_f | x_i, t_i)\exp(-G(x_f, t_f | x_i, t_i)),
\tag{74}
$$

where

$$
\begin{aligned}
&G(x_f, t_f | x_i, t_i) \\
&= \frac{1}{2}\left(\frac{(\mathcal{R}(x_f) - \mathcal{R}(x_i))^2}{t_f - t_i} - (\mathcal{M}(x_f) - \mathcal{M}(x_i))\right),
\end{aligned}
\tag{75}
$$

and $\mathcal{N}$ in Eq. (74) serves as the normalization constant, which is determined as

$$
\mathcal{N}(t_f | x_i, t_i) = \left(\int_{\mathcal{D}} \exp(-G(z, t_f | x_i, t_i))dz\right)^{-1},
\tag{76}
$$

where $\mathcal{D}$ denotes the domain of integration, accounting for any restrictions that $\mathcal{M}(\cdot)$ and $\mathcal{R}(\cdot)$ may impose.

References

1. Grigoriu, M.: Applied Non-Gaussian Processes: Examples, Theory, Simulation, Linear Random Vibration, and Matlab Solutions. Prentice Hall, Englewood Cliffs (1995)
2. Spanos, P.D., Zeldin, B.A.: Monte Carlo treatment of random fields: a broad perspective. Appl. Mech. Rev. **51**(3), 219–237 (1998)
3. Vanmarcke, E.: Random Fields: Analysis and Synthesis (Revised and Expanded New Edition). World Scientific, Singapore (2010)
4. Roberts, J.B., Spanos, P.D.: Random Vibration and Statistical Linearization. Courier Corporation, New York (2003)
5. Li, J., Chen, J.: Stochastic Dynamics of Structures. Wiley, New York (2009)
6. Grigoriu, M.: Stochastic Systems: Uncertainty Quantification and Propagation. Springer, London (2012)
7. Wiener, N.: The average of an analytic functional and the Brownian movement. Proc. Natl. Acad. Sci. **7**(10), 294–298 (1921)
8. Feynman, R.P.: Space-time approach to non-relativistic quantum mechanics. Rev. Mod. Phys. **20**(2), 367–387 (1948)
9. Di Matteo, A., Kougioumtzoglou, I.A., Pirrotta, A., Spanos, P.D., Di Paola, M.: Stochastic response determination of nonlinear oscillators with fractional derivatives elements via the Wiener path integral. Probab. Eng. Mech. **38**, 127–135 (2014)
10. Petromichelakis, I., Psaros, A.F., Kougioumtzoglou, I.A.: Stochastic response determination and optimization of a class of nonlinear electromechanical energy harvesters: a Wiener path integral approach. Probab. Eng. Mech. **53**, 116–125 (2018)
11. Psaros, A.F., Brudastova, O., Malara, G., Kougioumtzoglou, I.A.: Wiener path integral based response determination of nonlinear systems subject to non-white, non-Gaussian, and non-stationary stochastic excitation. J. Sound Vib. **433**, 314–333 (2018)
12. Psaros, A.F., Kougioumtzoglou, I.A., Petromichelakis, I.: Sparse representations and compressive sampling for enhancing the computational efficiency of the Wiener path integral technique. Mech. Syst. Signal Process. **111**, 87–101 (2018)
13. Meimaris, A.T., Kougioumtzoglou, I.A., Pantelous, A.A.: A closed form approximation and error quantification for the response transition probability density function of a class of stochastic differential equations. Probab. Eng. Mech. **54**, 87–94 (2018)
14. Meimaris, A.T., Kougioumtzoglou, I.A., Pantelous, A.A.: Approximate analytical solutions for a class of nonlinear stochastic differential equations. Eur. J. Appl. Math. 1–17 (2018) (In Press)
15. Grigoriu, M.: Stochastic Calculus: Applications in Science and Engineering. Springer, New York (2002)
16. Gardiner, C.: Stochastic Methods: A Handbook for the Natural and Social Sciences. Springer, New York (2009)
17. Risken, H.: The Fokker–Planck Equation: Methods of Solution and Applications. Springer, New York (1996)

18. Chaichian, M., Demichev, A.: Path Integrals in Physics: Volume I Stochastic Processes and Quantum Mechanics. CRC Press, Bath (2001)

19. Kougioumtzoglou, I.A., Spanos, P.D.: An analytical Wiener path integral technique for non-stationary response determination of nonlinear oscillators. Probab. Eng. Mech. **28**, 125–131 (2012)

20. Naess, A., Moe, V.: Stationary and non-stationary random vibration of oscillators with bilinear hysteresis. Int. J. Non-Linear Mech. **31**(5), 553–562 (1996)

21. Wehner, M.F., Wolfer, W.G.: Numerical evaluation of path-integral solutions to Fokker–Planck equations. II. Restricted stochastic processes. Phys. Rev. A **28**(5), 3003–3011 (1983)

22. Naess, A., Johnsen, J.M.: Response statistics of nonlinear, compliant offshore structures by the path integral solution method. Probab. Eng. Mech. **8**(2), 91–106 (1993)

23. Alevras, P., Yurchenko, D.: GPU computing for accelerating the numerical Path integration approach. Comput. Struct. **171**, 46–53 (2016)

24. Ewing, G.M.: Calculus of Variations with Applications. Dover Publications, New York (1969)

25. Kougioumtzoglou, I.A., Spanos, P.D.: Nonstationary stochastic response determination of nonlinear systems: a Wiener path integral formalism. ASCE J. Eng. Mech. **140**(9), 04014064: 1–14 (2014)

26. Kougioumtzoglou, I.A.: A Wiener path integral solution treatment and effective material properties of a class of one-dimensional stochastic mechanics problems. ASCE J. Eng. Mech. **143**(6), 04017014: 1–12 (2017)

27. Kougioumtzoglou, I.A., Di Matteo, A., Spanos, P.D., Pirrotta, A., Di Paola, M.: An efficient Wiener path integral technique formulation for stochastic response determination of nonlinear MDOF systems. J. Appl. Mech. **82**(10), 101005: 1–7 (2015)

28. Psaros, A.F., Petromichelakis, I., Kougioumtzoglou, I.A.: Wiener path integrals and multi-dimensional global bases for non-stationary stochastic response determination of structural systems. Mech. Syst. Signal Process. (Under Review) (2019)

29. Steele, J.M.: The Cauchy–Schwarz Master Class: An Introduction to the Art of Mathematical Inequalities. Cambridge University Press, New York (2004)

30. Roberts, J.B., Spanos, P.D.: Stochastic averaging: an approximate method of solving random vibration problems. Int. J. Non-Linear Mech. **21**(2), 314–333 (1986)

31. Spanos, P.D., Kougioumtzoglou, I.A., dos Santos, K.R.M., Beck, A.T.: Stochastic averaging of nonlinear oscillators: Hilbert transform perspective. ASCE J. Eng. Mech. **144**(2), 04017173: 1–9 (2018)

32. Kougioumtzoglou, I.A., Spanos, P.D.: An approximate approach for nonlinear system response determination under evolutionary stochastic excitation. Curr. Sci. **97**(8), 1203–1211 (2009)

33. Forsgren, A., Philip, E., Gill, P.E., Wright, M.H.: Interior methods for nonlinear optimization. SIAM Rev. **44**(4), 525–597 (2002)

34. Nocedal, J., Wright, S.J.: Numerical Optimization. Springer, New York (1999)

35. Macki, J.W., Nistri, P., Zecca, P.: Mathematical models for hysteresis. SIAM Rev. **35**(1), 94–123 (1993)

36. Bertotti, G., Mayergoyz, I.D.: The Science of Hysteresis: Mathematical Modeling and Applications, vol. I. Elsevier, New York (2003)

37. Ktena, A., Fotiadis, D.I., Spanos, P.D., Massalas, C.V.: A Preisach model identification procedure and simulation of hysteresis in ferromagnets and shape-memory alloys. Phys. B Condens. Matter **306**(1–4), 84–90 (2001)

38. Spanos, P.D., Cacciola, P., Red-Horse, J.: Random vibration of SMA systems via Preisach formalism. Nonlinear Dyn. **36**(2–4), 405–419 (2004)

39. Mayergoyz, I.D.: Mathematical Models of Hysteresis and Their Applications. Elsevier, New York (2003)

40. Ni, Y.Q., Ying, Z.G., Ko, J.M.: Random response analysis of Preisach hysteretic systems with symmetric weight distribution. ASME J. Appl. Mech. **69**(2), 171–178 (2002)

41. Spanos, P.D., Cacciola, P., Muscolino, G.: Stochastic averaging of Preisach hysteretic systems. ASCE J. Eng. Mech. **130**(11), 1257–1267 (2004)

42. Wang, Y., Ying, Z.G., Zhu, W.Q.: Stochastic averaging of energy envelope of Preisach hysteretic systems. J. Sound Vib. **321**(3–5), 976–993 (2009)

43. Kougioumtzoglou, I.A., Spanos, P.D.: Response and first-passage statistics of nonlinear oscillators via a numerical path integral approach. ASCE J. Eng. Mech. **139**, 1207–1217 (2013)

44. Kougioumtzoglou, I.A.: Stochastic joint time-frequency response analysis of nonlinear structural systems. J. Sound Vib. **332**, 7153–7173 (2013)

45. Spanos, P.D., Kougioumtzoglou, I.A.: Survival probability determination of nonlinear oscillators subject to evolutionary stochastic excitation. ASME J. Appl. Mech. **81**, 051016: 1–9 (2014)

46. Di Matteo, A., Spanos, P.D., Pirrotta, A.: Approximate survival probability determination of hysteretic systems with fractional derivative elements. Probab. Eng. Mech. **54**, 138–146 (2018)